Facile fabrication of ultralow-density transparent boehmite nanofiber cryogel beads and their application to a nanoglue

Gen Hayase*[a]

Abstract: Ultralow-density transparent porous bulk materials with densities of 5 mg cm^{-3} or less have only been obtained by supercritical drying. In this work, a simple method is reported for obtaining ultralow-density transparent porous beads with a diameter of several millimeters. In the method, a boehmite nanofiber dispersion (BNF sol) is dripped directly into liquid nitrogen and the beads are vacuum-dried. Normally, porous materials obtained via freeze drying exhibit strong light scattering due to structural nonuniformity and are not transparent. However, using dilute BNF as a skeleton structure suppressed the inhomogeneity due to aggregation during the dispersion medium crystallization. The lowest bulk density of the cryogel was 1.1 mg cm^{-3}, and the visible light transmittance reached 90 %. By dispersing functional materials into the BNF sol before freezing, composite materials were obtained. The facile method can be expected to develop the field of functional porous materials.

Aerogels have been researched intensively for over 80 years.[1] These structural materials are formed from a wide variety of compounds, including silica, alumina, titania, organic polymers, carbon materials, and biomaterials, which allows many possible applications.[2] A typical aerogel compound is silica. Silica aerogels have high visible-light transmittance, which is not observed in most other aerogels, and they have good thermal insulation properties when the density is around 150 mg cm^{-3}.[3] These properties mean that silica aerogels are expected to be used in smart windows.[2c, 4] In the physical sciences, the refractive index of low-density silica aerogels has been a focus of research.[5] By lowering the density of the silica aerogel, the refractive index can be brought close to air. To control of the optical properties further, ultralow-density transparent silica aerogels with a density of less than 5 mg cm^{-3} have been fabricated.[6] However, the fine skeleton structure composed of continuous spherical particles becomes brittle when the bulk density is lower; thus, more advanced techniques and a careful process are required to obtain crack-free aerogel monoliths. For this reason, there are few studies of ultralow-density transparent aerogels.

Recently, new techniques to form ultralow-density porous materials have been reported. Some of them are related to transparent or translucent monoliths. For example, Biener et al. prepared transparent nanotubular monoliths by atomic layer deposition templating.[7] In 2015, we obtained aerogels with high visible-light transmittance and ultralow refractive index by aggregating boehmite nanofibers (BNFs, AlOOH composition)[8] with diameters of several nanometers and an aspect ratio of 1000.[9] These aerogels had a visible-light transmittance of about 90 % through a thickness of 10 mm at densities of 5 mg cm^{-3} or less. Because the refractive index is close to that of air, objects placed on top of the aerogels appear to be “hovering”, depending on the background color (see the table of contents graphic in our previous paper[9]). The fine structure of the aerogels composed of BNFs, which are a one-dimensional material, is different from the continuous spherical particle structure in silica aerogels. The strength of BNF aerogels can be higher than silica aerogels because the nanofibers have no neck, which are a fracture point in the skeleton structure. In addition, for geometric reasons, nanofiber aerogels are lower density than continuous particle aerogels. Ultralow-density monoliths with compositions other than boehmite, such as copper oxide and titania, have been reported.[10] However, none of these ultralow-density nanofiber monoliths are transparent, which means that boehmite is special. Furthermore, the wet gel that is the basis of the ultralow-density BNF aerogel can be produced by a facile process of aggregating a commercially available BNF dispersion sol with a base. Boehmite nanofiber aerogels are highly reproducible because they do not require complicated reactions, and it is possible to prepare aerogels of any size and bulk shape after supercritical drying.

In this paper, a facile method for preparing ultralow-density transparent structures on the macroscale is reported. Instead of the conventional method of drying the wet gel with a supercritical fluid, ultralow-density porous materials were obtained by directly freezing the dispersed BNF sol and vacuum drying. Until now, various low-density monoliths have been produced by vacuum freeze drying, but they have all been opaque. During freeze drying, no surface tension acts on the gas-liquid interface during drying, and the monoliths are not shrunk by the capillary force. Consequently, low-density gels can be obtained easily by this drying method. However, when the sol is frozen, the dispersion medium (organic liquid) crystallizes and destroys the fine skeleton structure. To obtain transparent porous materials, it is necessary to eliminate structural heterogeneity on the scale of visible-light wavelengths (several hundreds of nanometers) or more, which is a source of Mie scattering, but the solvent crystals tend to grow larger. Therefore, it is almost impossible to obtain a transparent porous bulk structure by freeze drying. However, when the highly dispersed diluted BNF sol was instantly frozen (Movie S1), the skeleton structure had almost no aggregation, and a transparent cryogel of several millimeters was prepared.

The boehmite nanofiber cryogel was prepared as follows. A commercially available methyl isobutyl ketone (MIBK) dispersed BNF sol was diluted with *tert*-butyl alcohol (TBA). The

[a] Dr. Gen Hayase
Frontier Research Institute for Interdisciplinary Sciences
Tohoku University
6-3 Aramaki-aza Aoba, Aoba-ku, Sendai 980-8578, Japan.
E-mail: gen@aerogel.jp

Supporting information for this article is given via a link at the end of the document.

nanofibers used in this experiment had a diameter of several nanometers, an aspect ratio of 3000, and a specific surface area of approximately 350 m^2 g^{-1} for the dried nanofibers. The sol (5.5 µL) was dropped directly into liquid nitrogen with an electronic pipette. The sol was frozen instantly to form ~2 mm beads (Movie S1) that were vacuum dried for several hours. The frozen BNF sol, which was white at the time of freezing, became transparent gradually. After drying ultralow-density transparent cryogel beads were obtained (Movie S2).

Table 1 summarizes the starting compositions and the physical properties of the BNF cryogel beads, where the number in the sample names indicate the total mass when 1.0 g of 4.6 wt % BNF sol is diluted by adding TBA. The density decreased as the concentration of BNF in the starting sol decreased, and the transmittance increased. This is because the TBA and small amount of MIBK affect crystallization while the BNF sol droplet is being frozen, which means that the lower the concentration of dispersed nanofibers, the fewer aggregates are formed. **Figure 1** shows the transmittance at each wavelength with respect to the diameter of the beads obtained with each starting composition. The transmittance on the shorter wavelength side becomes smaller owing to the scattering. The visible-light transmittance of C75 was the highest, and it was confirmed by field-emission scanning electron microscopy (FESEM) that there was no dense aggregation of visible wavelength size in the nanofiber framework. **Figure 2** shows a digital photo and FESEM image of sample C75, and Movie S2 shows the change in appearance during freeze drying of C75. Almost no cryogel was visible at the end of the drying process. Changes in the bulk density of the cryogel were also examined. The minimum density was 1.1 mg cm^{-3}, observed for sample C75. As the BNF concentration decreased, the proportion of the skeleton in the bulk decreased and the material became unable to support its own weight, which resulted larger shrinkage after drying. For a BNF concentration of less than 0.45 g L^{-1} in the starting sol using TBA as a dispersion medium, the cryogel collapsed and lost its spherical shape. A similar experiment was carried out with water as the BNF dispersion medium, but all of the obtained beads were opaque (Figure S1). Since the crystal growth at the time of freezing, which causes coarsening of the microstructure, differs depending on the liquid, the dispersion medium is also important for forming a transparent porous structure.

Table 1. Properties of the BNF cryogel beads obtained from 5.5 µL of BNF sol.

Sample	BNF concentration in sol [g L^{-1}]	Volume of cryogel bead [µL]	Bulk density [mg cm^{-3}]	Visible-light transmittance at 550 nm [%]
C10	3.5	4.6 ± 0.4	4.2 ± 0.4	4.2
C25	1.4	3.8 ± 0.6	2.1 ± 0.4	22.6
C50	0.71	2.7 ± 0.5	1.3 ± 0.2	65.5
C75	0.48	2.3 ± 0.4	1.1 ± 0.2	91.1

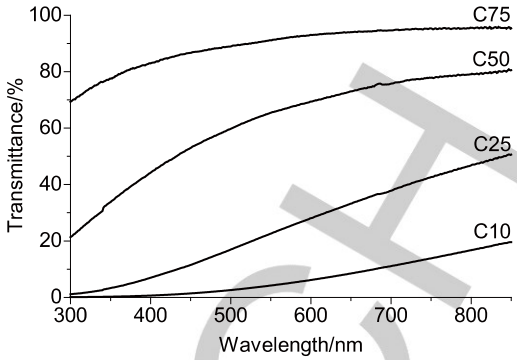

Figure 1. Light transmittance with respect to the penetration of the BNF cryogel bead center portion.

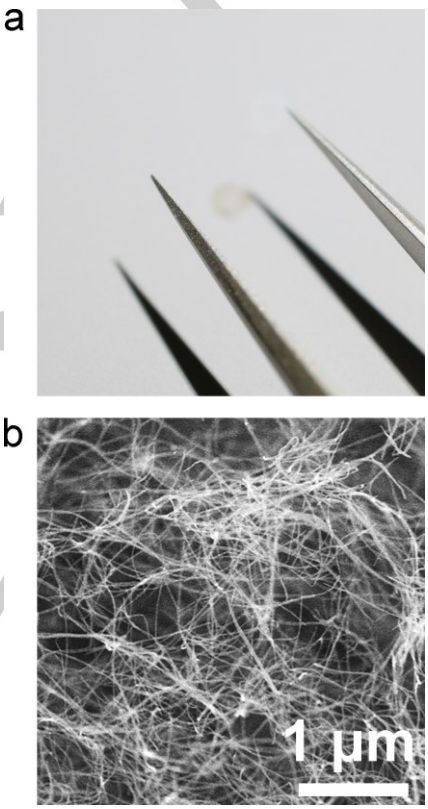

Figure 2. a) Photograph and b) FESEM image of the 2-mm BNF cryogel bead C75. The gel is too transparent to see, but can be confirmed by the shade.

Next, the applications of those transparent beads are discussed. Some researchers have reported functionalized materials that use transparent silica aerogels as a nanoglue and dispersing nanoparticles inside them.[11] These composite aerogels show optical characteristics and catalytic activities that depend on the composition of the dispersed material. In the present work, it was investigated whether BNF cryogels could produce similar composite materials as a host by adding guests such as fine particles, nanofibers, and functional molecules to the drops of BNF sol. Composite BNF cryogels were obtained with various dispersed materials. For example, a composite BNF

cryogel was obtained by dispersing microparticles of a commercially available phosphorescent pigment (LumiNova, Nemoto & Co., Ltd.) (**Figure 3**). Similarly, a composite obtained by dispersing the functional molecule diarylethene[12] showed photochromic properties. Adding carbon nanotubes (Figure S2) made the usually hydrophilic BNF cryogel beads water repellent, indicating that the surface properties were changed. The appearance of the BNF-composite beads varied from transparent to translucent. FESEM observation of the BNF-magnetic iron particle composite cryogel, which was attracted to magnets, showed that the particles were dispersed along the fiber without large aggregation (**Figure 4**). These results confirmed that the guest material was well dispersed in the BNF skeleton, thereby adding functionality. Currently, attempts to use BNF cryogel as a nanoglue are in the preliminary stages of functional material development, although it is expected that optical materials and sensors will be developed.

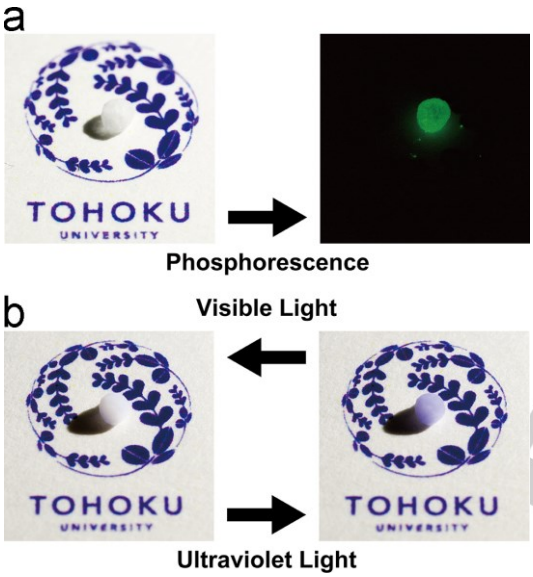

Figure 3. Photographs of BNF composite cryogel beads. a) BNF–phosphorescent pigment particle (LumiNova, Nemoto & Co., Ltd., average particle size ~ 60 μm), and b) BNF–diarylethene (1,2-Bis[2-methylbenzo[b]thiophen-3-yl]-3,3,4,4,5,5-hexafluoro-1-cyclopentene).

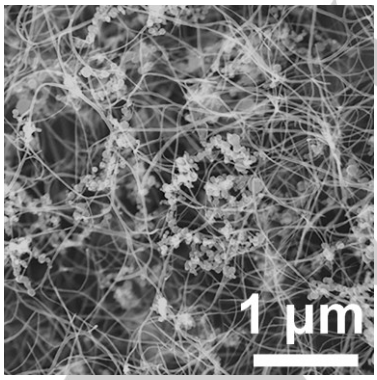

Figure 4. FESEM image of BNF–Fe_3O_4 particle (particle size is 50–100 nm) composite cryogel beads.

In summary, a sol with BNFs dispersed in TBA was dropped directly into liquid nitrogen and frozen, and then vacuum dried to obtain ultralow-density cryogel. It has previously been difficult to prepare transparent porous monoliths by vacuum freeze-drying because the uniformity of the skeleton structure is disturbed by crystallization of the dispersion medium, creating a scattering source. However, using a highly diluted BNF sol made nanofiber aggregation unlikely, and the beads became transparent like the aerogel obtained by supercritical drying. Although the ultralow-density transparent BNF cryogel is currently limited to beads, it is expected that a plate several millimeters thick will be developed. Adding a functional material to the BNF dispersion sol produced structures in which the functional material was dispersed among the nanofibers. In the future, a composite material with a BNF skeleton as a nanoglue could be used for optical materials and environmentally responsive sensor materials.[13]

Experimental Section

Experimental details can be found in the Supporting Information.

Acknowledgements

Financial support from a Grant-in-Aid for Scientific Research (KAKENHI, No. 15K17909) administrated by the Japan Society for the Promotion of Science (JSPS) and the Ministry of Education, Culture, Sports, Science and Technology (MEXT) (Japan). The author thanks Dr. Naofumi Nagai (Kawaken Fine Chemicals Co., Ltd.) for providing the BNF sol samples and their information.

Keywords: Gels • Nanostructures • Sol-gel processes

[1] a) S. S. Kistler, *Nature* **1931**, *127*, 741-741; b) H. D. Gesser, P. C. Goswami, *Chem. Rev.* **1989**, *89*, 765-788; c) J. Fricke, T. Tillotson, *Thin Solid Films* **1997**, *297*, 212-223; d) N. Hüsing, U. Schubert, *Angew. Chem., Int. Ed.* **1998**, *37*, 23-45.

[2] a) R. W. Pekala, C. T. Alviso, F. M. Kong, S. S. Hulsey, *J. Non-Cryst. Solids* **1992**, *145*, 90-98; b) M. Schneider, A. Baiker, *Catal. Today* **1997**, *35*, 339-365; c) A. C. Pierre, G. M. Pajonk, *Chem. Rev.* **2002**, *102*, 4243-4265; d) C. Moreno-Castilla, F. J. Maldonado-Hodar, *Carbon* **2005**, *43*, 455-465; e) I. Siro, D. Plackett, *Cellulose* **2010**, *17*, 459-494; f) G. Zu, J. Shen, X. Wei, X. Ni, Z. Zhang, J. Wang, G. Liu, *J. Non-Cryst. Solids* **2011**, *357*, 2903-2906.

[3] a) L. W. Hrubesh, R. W. Pekala, *J. Mater. Res.* **1994**, *9*, 731-738; b) D. M. Smith, A. Maskara, U. Boes, *J. Non-Cryst. Solids* **1998**, *225*, 254-259.

[4] a) L. W. Hrubesh, *J. Non-Cryst. Solids* **1998**, *225*, 335-342; b) M. Reim, W. Korner, J. Manara, S. Korder, M. Arduini-Schuster, H. P. Ebert, J. Fricke, *Sol. Energy* **2005**, *79*, 131-139.

[5] a) M. Cantin, M. Casse, L. Koch, R. Jouan, P. Mestreau, D. Roussel, F. Bonnin, J. Moutel, S. J. Teichner, *Nucl. Instrum. Methods* **1974**, *118*, 177-182; b) T. Sumiyoshi, I. Adachi, R. Enomoto, T. Iijima, R. Suda, M. Yokoyama, H. Yokogawa, *J. Non-Cryst. Solids* **1998**, *225*, 369-374.

[6] T. M. Tillotson, L. W. Hrubesh, *J. Non-Cryst. Solids* **1992**, *145*, 44-50.

[7] M. M. Biener, J. Ye, T. F. Baumann, Y. M. Wang, S. J. Shin, J. Biener, A. V. Hamza, *Adv. Mater.* **2014**, *26*, 4808-4813.

[8] a) N. Nagai, F. Mizukami, *J. Mater. Chem.* **2011**, *21*, 14884-14889; b) N. Nagai, Y.-h. Suzuki, C. Sekikawa, T. Y. Nara, Y. Hakuta, T. Tsunoda, F. Mizukami, *J. Mater. Chem.* **2012**, *22*, 3234-3241.

[9] G. Hayase, K. Nonomura, G. Hasegawa, K. Kanamori, K. Nakanishi, *Chem. Mater.* **2015**, *27*, 3-5.

[10] a) J. Zou, J. Liu, A. S. Karakoti, A. Kumar, D. Joung, Q. Li, S. I. Khondaker, S. Seal, L. Zhai, *ACS Nano* **2010**, *4*, 7293-7302; b) S. M. Jung, H. Y. Jung, M. S. Dresselhaus, Y. J. Jung, J. Kong, *Sci. Rep.* **2012**, *2*, 849; c) Y. Tang, K. L. Yeo, Y. Chen, L. W. Yap, W. Xiong, W. Cheng, *J. Mater. Chem. A* **2013**, *1*, 6723-6726; d) H. Sun, Z. Xu, C. Gao, *Adv. Mater.* **2013**, *25*, 2554-2560; e) S. M. Jung, H. Y. Jung, W. Fang, M. S. Dresselhaus, J. Kong, *Nano Lett.* **2014**, *14*, 1810-1817; f) J. P. Zhang, B. C. Li, L. X. Li, A. Q. Wang, *J. Mater. Chem. A* **2016**, *4*, 2069-2074.

[11] a) C. A. Morris, M. L. Anderson, R. M. Stroud, C. I. Merzbacher, D. R. Rolison, *Science* **1999**, *284*, 622-624; b) F. J. Heiligtag, W. Cheng, V. R. d. Mendonça, M. J. Süess, K. Hametner, D. Günther, C. Ribeiro, M. Niederberger, *Chem. Mater.* **2014**, *26*, 5576-5584.

[12] M. Irie, K. Uchida, *Bull. Chem. Soc. Jpn.* **1998**, *71*, 985-996.

[13] D. L. Plata, Y. J. Briones, R. L. Wolfe, M. K. Carroll, S. D. Bakrania, S. G. Mandel, A. M. Anderson, *J. Non-Cryst. Solids* **2004**, *350*, 326-335.